

## Lasing of donor-bound excitons in ZnSe microdisks

A. Pawlis,<sup>1,2,\*</sup> M. Panfilova,<sup>1</sup> D. J. As,<sup>1</sup> K. Lischka,<sup>1</sup> K. Sanaka,<sup>2</sup> T. D. Ladd,<sup>2</sup> and Y. Yamamoto<sup>2</sup>

<sup>1</sup>*Department of Physics, University of Paderborn, Warburger Strasse 100, 33098 Paderborn, Germany*

<sup>2</sup>*Edward L. Ginzton Laboratory, Stanford University, Stanford, California 94305-4088, USA*

*and National Institute of Informatics, 2-1-2 Hitotsubashi, Chiyoda-ku, Tokyo 101-8430, Japan*

(Received 6 March 2008; published 18 April 2008)

Excitons bound to fluorine atoms in ZnSe have the potential for several quantum optical applications. Examples include optically accessible quantum memories for quantum information processing and lasing without inversion. These applications require the bound-exciton transitions to be coupled to cavities with high cooperativity factors, which results in the experimental observation of low-threshold lasing. We report such lasing from fluorine-doped ZnSe quantum wells in 3 and 6  $\mu\text{m}$  microdisk cavities. Photoluminescence and selective photoluminescence spectroscopy confirm that the lasing is due to bound-exciton transitions.

DOI: [10.1103/PhysRevB.77.153304](https://doi.org/10.1103/PhysRevB.77.153304)

PACS number(s): 78.55.Et, 03.67.-a, 42.55.Sa, 78.67.-n

Quantum interference of the two optical pathways of an optical  $\Lambda$  system, in which two long-lived ground states are optically coupled to a single excited state, provides a powerful mechanism for a number of useful applications. These applications include lasing without inversion,<sup>1</sup> electromagnetically induced transparency,<sup>2</sup> and optically addressable quantum memory for quantum information processing.<sup>3–8</sup> The development of scalable technologies based on these effects would be facilitated by solid-state implementations, which are generally more difficult than the atomic demonstrations due to optical inhomogeneity and decoherence.

In semiconductors, donor impurities and charged quantum dots both provide promising realizations of such  $\Lambda$  systems. The long-lived ground states are provided by the bound electron spin in high magnetic field, while the optically excited state is formed by the lowest-energy donor-bound exciton or trion state. For applications involving quantum memory, however, quantum dots have the disadvantage of severe inhomogeneity in optical transition frequencies and electron magnetic moments. Such inhomogeneity may inhibit the ability to incorporate many optically interacting quantum-dot-based  $\Lambda$  systems into a scalable quantum-information-processing device. In contrast, the potentials provided by the donor impurities in a perfect crystal are very homogeneous, as demonstrated by high-quality samples of GaAs (Ref. 9) and Si.<sup>10</sup> Homogeneous ensembles of donor-bound excitons in bulk GaAs have been demonstrated to exhibit coherent-population trapping,<sup>11</sup> which is one effect that exhibits quantum coherence between the two emission pathways of the optical  $\Lambda$  system.

Donor-bound excitons in ZnSe are of particular interest because ZnSe may be isotopically purified to feature only spin-0 substrate nuclei, avoiding the disadvantage of decoherence limited by the dynamics of nuclear spins in III–V semiconductor systems.<sup>12</sup> Silicon-based systems also have the potential to overcome nuclear decoherence,<sup>13</sup> but silicon is optically dark due to its indirect band gap. In a II–VI system such as ZnSe, the nuclear spins may be entirely removed from the substrate as in the case in silicon, and the donor-bound-exciton emission is optically bright as in the case of GaAs. The fluorine donor is of particular interest because it provides a 100% abundant spin-1/2 nucleus,

which may be employed for long-lived storage of quantum information.

ZnSe is a wide-band-gap semiconductor which emits light in the blue region ( $\lambda \approx 440$  nm), where lasing is traditionally difficult to obtain. Early studies of lasing in ZnSe for the purpose of blue lasers were limited because the material is too soft to be used in high-current or high-excitation regimes, so that heating effects degenerate the active medium.<sup>14,15</sup> However, low-threshold lasing is achievable when a high- $Q$ , low-volume optical microcavity introduces a high ratio of stimulated emission to spontaneous emission, known as the  $\beta$  factor.<sup>16</sup> Such low-threshold lasing is seen in recent developments in microcavity quantum dot lasers.<sup>17</sup> Further, if the lasing medium is provided by discrete donor-bound-exciton transitions rather than the continuum of free excitons, the coherence provided by the spin-ground states of the donor spins could allow the possibility of lasing without inversion,<sup>1</sup> further decreasing the input power requirements.

Lasing in ZnSe donor-bound excitons may be particularly useful as a component in quantum information processing devices. The design of quantum computers<sup>7</sup> or quantum repeaters<sup>8</sup> based on donor-bound excitons in optical microcavities requires a low-noise source laser nearly resonant the bound-exciton transitions used for qubit initialization, control, and readout. A laser based on the same medium as the qubit provides promising pathways for device integration.

Bound-exciton emission in ZnSe was observed many years ago,<sup>18</sup> and the optical transitions of single, isolated ZnSe acceptors were recently measured.<sup>19</sup> However, coherent applications involving  $\Lambda$  systems are more likely to be achieved from donors due to the longer coherence time of electrons over holes. The <sup>19</sup>F donor has been studied earlier in bulk samples.<sup>20</sup> In this Brief Report, we report evidence of <sup>19</sup>F donors optically coupled to microcavities exhibiting low-threshold lasing of the donor-bound-exciton transitions.

Previous work on microcavity lasers in the wide-band-gap II–VI semiconductors has focused on lasers based on CdSe quantum dots<sup>21,22</sup> or ZnCdSe quantum wells (QWs)<sup>23</sup> confined by quaternary alloys of ZnMgSSe and ZnCdSSe, which are lattice matched to a GaAs substrate. To reduce alloy fluctuations, we confined a ZnSe QW in ternary ZnMgSe barriers with low Mg concentration. Lasing due to confined free

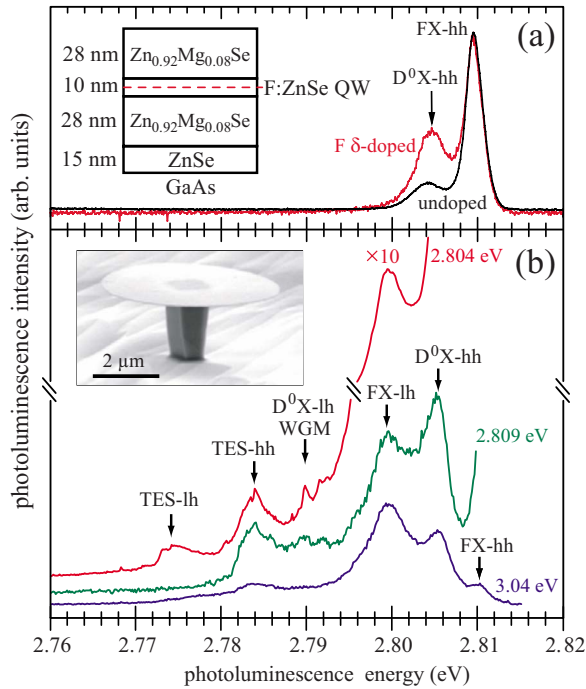


FIG. 1. (Color online) PL and SPL spectra taken at 5 K. (a) PL for unstructured F:ZnSe  $\delta$ -doped QW (red or gray curve) and undoped QW (black curve). Inset: the material composition of the unstructured sample. (b) Above-band PL (blue or black curve) and SPL spectra of a 6  $\mu\text{m}$  disk taken under resonant excitation of the  $D^0X$ -hh peak (laser energy of 2.804 eV) and the FX-hh peak (laser energy of 2.809 eV). Inset: scanning electron micrograph of a 6  $\mu\text{m}$  disk.

excitons seeded by excitonic molecules has been previously observed in similar systems.<sup>24,25</sup> Here, we show lasing directly on discrete, bound-exciton transitions in samples with a fluorine  $\delta$ -doped ( $^{19}\text{F}$ :ZnSe) layer at the center of the QW.

The ZnMgSe/ZnSe/ $^{19}\text{F}$ :ZnSe/ZnSe/ZnMgSe samples were grown by molecular beam epitaxy on GaAs-(001) substrates. For optimal interface properties, a 15 nm buffer of undoped ZnSe was first deposited on the substrate, followed by 28 nm of ZnMgSe with Mg content of about 8%. The ZnSe QW was 10 nm thick. For doped samples, the QW was  $\delta$  doped in the center by using a  $\text{ZnF}_2$  evaporation cell with a net molecular flux of approximately  $2 \times 10^9 \text{ cm}^{-2} \text{ s}^{-1}$ , which is equivalent to a sheet donor concentration of  $8 \times 10^9 \text{ cm}^{-2}$ .

Photoluminescence (PL) spectra of unstructured  $^{19}\text{F}$ -doped and undoped samples were measured at 5 K, with excitation provided by a blue light-emitting diode with wavelength of 365 nm [Fig. 1(a)]. The PL spectra of these strained samples show two peaks. The emission at 2.810 eV corresponds to the recombination of heavy-hole free excitations (FX-hh) from the compressively strained ZnSe QW [lattice mismatch of  $f(\text{ZnSe}) = -0.25\%$ ]; this energy is consistent with the finite barrier model in Refs. 27 and 28.

Light-hole free-exciton (FX-lh) emission at 2.829 eV is not observed at low temperature. The lower-energy peak seen at 2.804 eV in Fig. 1 is due to the heavy-hole donor-bound-exciton ( $D^0X$ -hh) recombination, as confirmed by the expected 6 meV separation and the threefold increase in this

line provided by the fluorine  $\delta$ -doped (red or gray curve) versus the undoped sample (black curve).

The widths of these peaks indicate inhomogeneous broadening likely due to strain effects. However, the broadening is still less than typically seen in ensembles of quantum dots and may be useful for the isolation of individual impurities.

Microdisks with diameters of 3 and 6  $\mu\text{m}$  were defined by photolithography, reactive ion etching, and wet etching of the underlying GaAs substrate. The inset of Fig. 1(b) shows a scanning electron micrograph picture of such a microdisk. The absence of cracks and lateral deformation indicates a homogeneous release of strain along the radial direction of the disks; however, considering the volume ratio of ZnMgSe versus ZnSe in the disks, the ZnSe QW is likely to be tensile strained on ZnMgSe in the periphery of the disks. This results in a substantial band gap narrowing effect along the radial direction of the disk from the center to the edge, which enhances the charge carrier transfer to the periphery, where the optical whispering gallery modes (WGMs) are localized. As a result of the tensile strain, the relative positions of the FX-lh and FX-hh energies are reversed and both states contribute to the PL.

Band-gap narrowing and strain relaxation are confirmed by the corresponding PL-spectrum in Fig. 1(b) taken from a microdisk with 6  $\mu\text{m}$  diameter. The modified transition energies are found by fitting the above-band PL to five Gaussian peaks. These energies are again consistent with the finite barrier model reported in Refs. 26 and 27 with a remaining induced tensile lattice mismatch of the quantum well of  $f(\text{ZnSe}) = +0.2\%$  in the etched structure.

The FX-hh and  $D^0X$ -hh transitions at 2.81 and 2.804 eV are only slightly shifted and broadened; these peaks come from PL around the center of the disk, where the material remains fully strained. No cavity modes are ever observed in this region of the spectrum. The  $D^0X$ -hh luminescence is now stronger than the FX-hh luminescence due to surface recombination of the FX, and satellite transitions are now visible at a position of 21 meV beneath the  $D^0X$ -hh luminescence. This energy is in agreement with the calculated position of the two electron satellite (TES) of the  $D^0X$ .<sup>28</sup> In the relaxed periphery, the FX-lh emission moves to the lower-energy position of about 2.799 eV; the  $D^0X$  transitions again appear 6 meV lower than their corresponding FX transitions, but are substantially broadened due to the strain gradient across the disk.

The association of the spectral peaks in structured samples is also confirmed by selective photoluminescence (SPL), in which the FX-hh transition and the  $D^0X$ -hh transition are resonantly excited by a scanning narrow-band Ti:sapphire ring laser doubled by an LiNBO crystal in a high-finesse cavity. Figure 1(b) shows the SPL spectra of a 6  $\mu\text{m}$  microdisk. By resonant excitation of the FX-hh transition at 2.809 eV (green or dark gray curve), the TES-hh lines are enhanced relative to above-band excitation. Resonant excitation of the  $D^0X$ -hh peak (red or light gray curve) results in the appearance of a new satellite peak at 2.774 eV which we identify as the TES-lh transitions. These observations of TES lines in SPL strongly confirm the expected contribution of F-donor-bound excitons to the band-edge luminescence, as opposed to emission from quantum dots due to surface fluc-

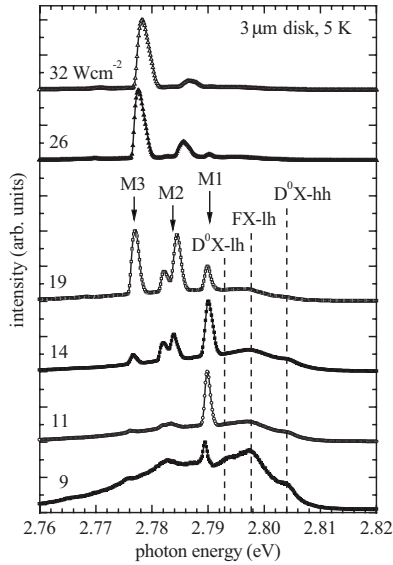


FIG. 2. Power-dependent PL spectra and lasing of a microdisk with 3  $\mu\text{m}$  diameter. The excitation density was varied between 9 and 32  $\text{W cm}^{-2}$ . For low excitation, the WGM (mode M1) emerges at 2.790 eV. The energies of the relevant heavy-hole and light-hole transitions are indicated by dashed lines. Further modes (M2 and M3) are observed at moderate excitation densities.

tuations of the QW. We also repeatedly observe a sharp peak at 2.79 eV when resonantly exciting the  $D^0X$ -hh line. This peak corresponds to a WGM of the microdisk.

The WGM modes are enhanced with high-power pumping. Figure 2 shows a series of PL spectra taken from a microdisk with 3  $\mu\text{m}$  diameter and measured with different average excitation intensities varying between 9 and 32  $\text{W cm}^{-2}$ . For small power densities exceeding 5  $\text{W cm}^{-2}$ , superlinear increase in a sharp peak at 2.790 eV (mode M1 in Fig. 2) is observed. This peak corresponds to a WGM of the microdisk excited by  $D^0X$ -lh emission. The linewidth indicates a cavity  $Q$  of about 2500. Additional modes emerge at energies of 2.783 and 2.785 eV (mode M2) and at 2.776 eV (mode M3) for pump power densities larger than 12  $\text{W cm}^{-2}$ . These modes are too closely spaced to correspond to the free spectral range of the lowest order WGMs; the multiple modes seen are likely due to higher order radial modes of the disk. The strain gradient and slight warping of these disks prevent a simple quantitative evaluation of their spacing. Mode M2 consists of two competing modes close to each other which might stem from anisotropy of the disk shape. At higher-excitation density, the overall intensity of mode M1 and mode M2 is transferred to mode M3, which is resonant with the TES transition energies of the bound-exciton states. The WGMs are only observed in the lower-energy part of the spectra corresponding to emission from donor-bound excitons and their related transitions, resulting from the band-gap narrowing at the periphery of the disk.

The peaks corresponding to WGMs are not visible in low-power PL by using either a continuous wave 405 nm diode laser or the doubled 408 nm output of a mode-locked Ti:sapphire laser. We believe that this is because absorption due to lower-energy transitions in the inhomogeneously broadened distribution damps the cavity  $Q$ . However, at higher-

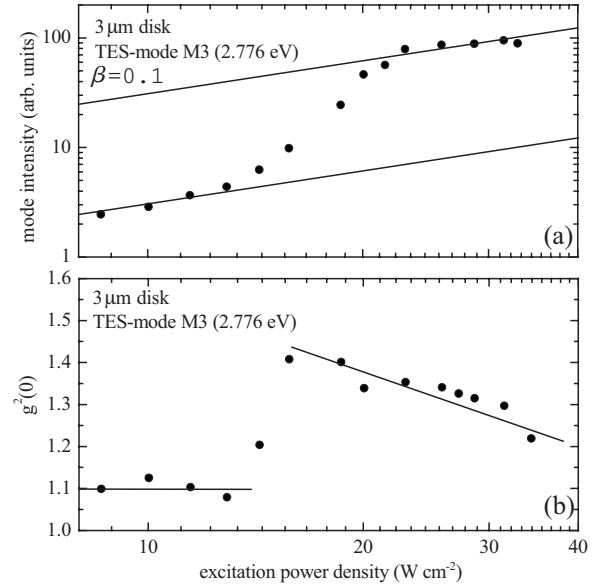


FIG. 3. (a) Integrated intensity of the TES lasing mode M3 at 2.776 eV versus the excitation power density. (b) Power-dependent second-order photon correlation measured on mode M3.

excitation powers, these lower-energy transitions become saturated and the cavity modes appear.

Figure 3(a) shows the power dependence of mode M3 as a function of the pump power. A clear lasing threshold is seen at about 15  $\text{W cm}^{-2}$ . This threshold is substantially smaller than observed in previous II-VI-semiconductor microdisk lasers based on quantum dots.<sup>22</sup> The ratio of the slope of the output power versus input power indicates the fraction of spontaneous emission coupled into the lasing mode to be  $\beta=0.1$ . Lasing was also observed in 6  $\mu\text{m}$  microdisks, revealing threshold power densities larger than 100  $\text{W cm}^{-2}$  for the TES transition with a corresponding  $\beta$  factor of about 0.03.

Lasing was confirmed by the power dependence of the second-order photon correlation function  $g^{(2)}(0)$ , which is measured at the TES lasing mode M3 with a standard Hanbury-Brown Twiss (HBT) experiment and shown in Fig. 3(b). Below threshold, the spontaneous emission into mode M3 follows a nearly Poisson distribution with  $g^{(2)}(0) \approx 1.1$ . Near threshold, we observe significant photon bunching, manifested as  $g^{(2)}(0) > 1$ . Such bunching occurs as the coherence length of the photons increases near threshold but before the fully coherent output of above-threshold lasing. Far above threshold (powers exceeding 30  $\text{W cm}^{-2}$ ), the HBT signal converges back to  $g^{(2)}(0) \approx 1$ , indicating the generation of a coherent state.

The observed  $\beta$  factors allow us to estimate the cooperativity factors of the microdisk cavities. In microdisks, such as these that are very wide and very thin relative to the emission wavelength, the spontaneous emission rate into all cavity modes including unguided modes sum to very nearly the spontaneous emission rate in the bulk. Therefore, the  $\beta$  factor for one of the WGMs is approximately  $\beta=(1+C)\beta_0$ , where  $\beta_0$  is the ratio of the emission rate into a vanishing- $Q$  WGM normalized by the bulk emission rate and the cooperativity factor  $C$  manifests as the Purcell effect.

We estimate the mode volume  $\beta_0$  by using the approximation presented in Ref. 29 in the large-radius limit. We find that for disks as thin as these, the WGMs are quite wide, allowing about 500 impurities to contribute to the lasing in a 3  $\mu\text{m}$  disk. This model yields  $\beta_0 \approx 0.02$ , for an expected cooperativity factor of about  $C=4$ , which is consistent with estimates based on a  $Q$  of 2500 and the calculated mode volume. Both  $C$  and  $\beta_0$  inversely scale with the disk radius, consistent with the smaller observed  $\beta$  factor of the 6  $\mu\text{m}$  disk.

The appearance of low-threshold lasing in  $\delta$ -doped  $^{19}\text{F}:\text{ZnSe}$  QW microdisks indicates that small ensembles of  $^{19}\text{F}$  donors have been successfully coupled to a cavity with

cooperativity factors high enough to allow some schemes for quantum communication and quantum computation.<sup>8</sup> The reduction in inhomogeneous broadening by preserving the uniform strain acquired during molecular beam epitaxy growth may allow such applications as lasing without inversion. Further work will involve the isolation of individual impurities in smaller microcavities, the measurement of the donor-spin coherence times, and the measurement of single  $^{19}\text{F}$  nuclear spin states.

This work was supported by NICT. We thank Kristiaan De Greve and Shinichi Koseki for valuable discussions and experimental assistance.

\*pawlis@stanford.edu

- <sup>1</sup>M. O. Scully and M. Fleischhauer, *Science* **263**, 337 (1994).
- <sup>2</sup>S. E. Harris, J. E. Field, and A. Imamoglu, *Phys. Rev. Lett.* **64**, 1107 (1990).
- <sup>3</sup>J. I. Cirac, P. Zoller, H. J. Kimble, and H. Mabuchi, *Phys. Rev. Lett.* **78**, 3221 (1997).
- <sup>4</sup>W. Yao, R.-B. Liu, and L. J. Sham, *Phys. Rev. Lett.* **95**, 030504 (2005).
- <sup>5</sup>L. I. Childress, J. M. Taylor, A. Sørensen, and M. D. Lukin, *Phys. Rev. A* **72**, 052330 (2005).
- <sup>6</sup>E. Waks and J. Vuckovic, *Phys. Rev. Lett.* **96**, 153601 (2006).
- <sup>7</sup>S. M. Clark, Kai-Meis C. Fu, T. D. Ladd, and Y. Yamamoto, *Phys. Rev. Lett.* **99**, 040501 (2007).
- <sup>8</sup>T. D. Ladd, P. van Loock, K. Nemoto, W. J. Munro, and Y. Yamamoto, *New J. Phys.* **8**, 184 (2006).
- <sup>9</sup>V. A. Karasyuk, D. G. S. Beckett, M. K. Nissen, A. Villemaire, T. W. Steiner, and M. L. W. Thewalt, *Phys. Rev. B* **49**, 16381 (1994).
- <sup>10</sup>A. Yang, M. Steger, D. Karauskaj, M. L. W. Thewalt, M. Cardona, K. M. Itoh, H. Riemann, N. V. Abrosimov, M. F. Churbanov, A. V. Gusev *et al.*, *Phys. Rev. Lett.* **97**, 227401 (2006).
- <sup>11</sup>K. M. C. Fu, C. Santori, C. Stanley, M. C. Holland, and Y. Yamamoto, *Phys. Rev. Lett.* **95**, 187405 (2005).
- <sup>12</sup>R. de Sousa and S. Das Sarma, *Phys. Rev. B* **68**, 115322 (2003).
- <sup>13</sup>A. M. Tyryshkin, S. A. Lyon, A. V. Astashkin, and A. M. Raitsimring, *Phys. Rev. B* **68**, 193207 (2003).
- <sup>14</sup>L. L. Chao, G. S. C. III, C. Kothandaraman, T. Marshall, E. Snoeks, M. Buijs, K. Haberern, J. Petruzzello, G. M. Haugen, and K. K. Law, *Appl. Phys. Lett.* **70**, 535 (1997).
- <sup>15</sup>H. Okuyama, *IEICE Trans. Electron.* **E83-C**, 536 (2000).
- <sup>16</sup>Y. Yamamoto, S. Machida, and G. Björk, *Phys. Rev. A* **44**, 657 (1991).
- <sup>17</sup>S. Strauf, K. Hennessy, M. T. Rakher, Y.-S. Choi, A. Badolato, L. C. Andreani, E. L. Hu, P. M. Petroff, and D. Bouwmeester, *Phys. Rev. Lett.* **96**, 127404 (2006).
- <sup>18</sup>J. L. Merz, H. Kukimoto, K. Nassau, and J. W. Shiever, *Phys. Rev. B* **6**, 545 (1972).
- <sup>19</sup>S. Strauf, P. Michler, M. Klude, D. Hommel, G. Bacher, and A. Forchel, *Phys. Rev. Lett.* **89**, 177403 (2002).
- <sup>20</sup>A. Pawlis, K. Sanaka, S. Götzinger, Y. Yamamoto, and K. Lischka, *Semicond. Sci. Technol.* **21**, 1412 (2006).
- <sup>21</sup>J. Renner, L. Worschech, A. Forchel, S. Mahapatra, and K. Brunner, *Appl. Phys. Lett.* **89**, 091105 (2006).
- <sup>22</sup>J. Renner, L. Worschech, A. Forchel, S. Mahapatra, and K. Brunner, *Appl. Phys. Lett.* **89**, 231104 (2006).
- <sup>23</sup>M. Hovinen, J. Ding, A. V. Nurmikko, D. C. Grillo, J. Han, L. He, and R. L. Gunshor, *Appl. Phys. Lett.* **63**, 3128 (1993).
- <sup>24</sup>F. Kreller, M. Lowisch, J. Puls, and F. Henneberger, *Phys. Rev. Lett.* **75**, 2420 (1995).
- <sup>25</sup>V. Kozlov, P. Kelkar, A. V. Nurmikko, C.-C. Chu, D. C. Grillo, J. Han, C. G. Hua, and R. L. Gunshor, *Phys. Rev. B* **53**, 10837 (1996).
- <sup>26</sup>K. L. Teo, Y. P. Feng, M. F. Li, T. C. Chong, and J. B. Xia, *Semicond. Sci. Technol.* **9**, 349 (1994).
- <sup>27</sup>T.-Y. Chung, J. H. Oh, S.-G. Lee, J.-W. Jeong, and K. J. Chang, *Semicond. Sci. Technol.* **12**, 701 (1997).
- <sup>28</sup>P. J. Dean, D. C. Herbert, C. J. Werkhoven, B. J. Fitzpatrick, and R. N. Bhargava, *Phys. Rev. B* **23**, 4888 (1981).
- <sup>29</sup>M. K. Chin, D. Y. Chu, and S.-T. Ho, *J. Appl. Phys.* **75**, 3302 (1994).